OPTICAL METHODS FOR PERFORMANCE EVALUATION OF TWO-DIMENSIONAL TRANSONIC TURBINE PROFILES IN STEAM

by

R. DECUYPERE
Ecole Royale Militaire
Laboratoire de Mécanique Appliquée
30 avenue de la Renaissance - 1040
Bruxelles

and

A. ARTS
Von Karman Institute for Fluid Dynamics
72 Chaussée de Waterloo
1640 Rhode Saint Genese
Belgique

1. Introduction

For some years a two-dimensional steam tunnel exists at the Applied Mechanics Laboratory of the Royal Military Academy of Belgium. A description of the tunnel is given in Ref 1 and 2. The aim of this contribution is to explain how optical methods, which are standard techniques for performance evaluation of turbomachine blades in air tunnels can be used when the fluid is steam.

A two-dimensional cascade of typical steam turbine tip section profiles of a last stage rotor was placed in the test section of the tunnel. Two visualization methods are applied : Schlieren and interferometry which are essentially qualitative methods. To quantify the cascade performance a laser-velocimeter is used.

2. Visualization of density gradients

While in air tunnels the requirements of the test section windows are relatively modest, some additional conditions must be fulfilled when making visualizations in steam :

- the optical properties must be maintained at high temperature
- the windows must withstand strong temperature gradients. As a matter of fact, the test section temperature may be as high as 250°C, while the other side of the window is at ambient temperature
- they must also resist to high temperature variations occurring especially when starting the facility
- the windows must withstand pressure forces in both senses because the test section pressure may be above or below the ambient pressure
- it should be possible to drill holes or grooves to fix the blades without having exagerated local stresses

On top of that, the fixation of the windows in the tunnel side walls should :

- exclude clearances with the blade ends at any temperature
- control the stresses exerted on the windows by thermal dilatation of the blades along the span and by deformation of the tunnel side walls.

Perspex windows, which are very cheap and easy to shape giving complete satisfaction in flow visualization techniques in air tunnels, cannot withstand steam. As a matter of fact already at 80°C, perspex is loosing its hardness while its thermal dilatation is very important so that plastic deformation occurs. Ordinary glass cannot withstand important local temperature gradients nor the temperature variations occurring when starting the tunnel.

lowed by a beam expander, increasing the diameter of the incident laser beam entering the focussing lens by a factor 2.27. As a result of this, the measuring volume diameter is decreased by a factor 2.27 while the length is decreased by 5 and the S/N increased by about 5. However the beam distance is also increased by 2.27 resulting in 15 μm wide fringes when a focussing lens of 600 mm focal distance is used (Fig 6).

c. Receiving optics.

Forward scattering is used to provide the best S/N especially for the high velocities we are dealing with. To avoid scattering light from reflections of the incident beams on the windows, the "on-axis" position of the photomultiplier is not advisable, especially for the small angle of the beams, which is only 2°. With respect to the optical axis, the photomultiplier is placed at 24°.

As to our experience, only satisfactory results could be obtained with fused silica windows. As a matter of fact due to the density gradients of pyrex, the photomultiplier could not be kept centered on the probe volume when the velocimeter platform was moved around the cascade.

d. Signal generation

As superheated steam does not contain any particles and because in wet steam the droplets are too small to provide acceptable signals, the flow must be seeded.

To avoid dirtying the windows by oil or other liquids giving rise to deposits, and agglomeration of solid particles in the condensor, the flow is seeded with water droplets. A two millimeter thick tube is inserted in the settling chamber. The tube head presents a small nozzle of 0.6, 0.3 or 0.1 mm diameter producing a spray of water droplets supplied from outside the tunnel. For convenience these nozzles are denominated N6, N3 and N1

e. Signal processing

Signal processing is performed by the TSI 1980A counter. The digital output (time for N cycles, minimum cycles per burst, data ready, data hold) is interfaced with a 8 bits minicomputer. To allow fast data transmission, four VIA 6522 are added to the computer, allowing multiple devices to be connected.

3.2 Selection of the nozzle type.

First of all it was examined in which measure the droplets generated by the three nozzles follow the steam flow. Therefore measurements were carried out in points A and B of Fig 7. Station A (x=6032) is located 18 % of chord length upstream of the leading edge plane, so that the flow conditions are uniform. Fig 8 shows the histograms for the three nozzles. The TSI counter is equipped with an amplitude discriminator to avoid signals from large particles to be processed. For each nozzle two histograms are shown. The first histogram was obtained with the discriminator in the off position. All signals are applied to the validation unit. For all nozzles, the second histogram corresponds to an identical position of the amplitude discriminator eliminating signals with high pedestal. These diagrams show that in station A the mean velocity is not affected by amplitude discrimination. The slight differences are within the influence of inlet total pressure which was not exactly constant for these tests. The velocity increase realized in the converging nozzle between the settling chamber and the test section is smooth so that the influence of inertia of droplets with different sizes is limited. When amplitude discrimination is used the only effect seems to be a slight drop in deviation.

Station B is located in front of the upwards going trailing edge shock. Due to important acceleration in the

lowed by a beam expander, increasing the diameter of the incident laser beam entering the focussing lens by a factor 2.27. As a result of this, the measuring volume diameter is decreased by a factor 2.27 while the length is decreased by 5 and the S/N increased by about 5. However the beam distance is also increased by 2.27 resulting in 15 μm wide fringes when a focussing lens of 600 mm focal distance is used (Fig 6).

c. Receiving optics.

Forward scattering is used to provide the best S/N especially for the high velocities we are dealing with. To avoid scattering light from reflections of the incident beams on the windows, the "on-axis" position of the photomultiplier is not advisable, especially for the small angle of the beams, which is only 2°. With respect to the optical axis, the photomultiplier is placed at 24°.

As to our experience, only satisfactory results could be obtained with fused silica windows. As a matter of fact due to the density gradients of pyrex, the photomultiplier could not be kept centered on the probe volume when the velocimeter platform was moved around the cascade.

d. Signal generation

As superheated steam does not contain any particles and because in wet steam the droplets are too small to provide acceptable signals, the flow must be seeded.

To avoid dirtying the windows by oil or other liquids giving rise to deposits, and agglomeration of solid particles in the condensor, the flow is seeded with water droplets. A two millimeter thick tube is inserted in the settling chamber. The tube head presents a small nozzle of 0.6, 0.3 or 0.1 mm diameter producing a spray of water droplets supplied from outside the tunnel. For convenience these nozzles are denominated N6, N3 and N1

e. Signal processing

Signal processing is performed by the TSI 1980A counter. The digital output (time for N cycles, minimum cycles per burst, data ready, data hold) is interfaced with a 8 bits minicomputer. To allow fast data transmission, four VIA 6522 are added to the computer, allowing multiple devices to be connected.

3.2 Selection of the nozzle type.

First of all it was examined in which measure the droplets generated by the three nozzles follow the steam flow. Therefore measurements were carried out in points A and B of Fig 7. Station A (x=6032) is located 18 % of chord length upstream of the leading edge plane, so that the flow conditions are uniform. Fig 8 shows the histograms for the three nozzles. The TSI counter is equipped with an amplitude discriminator to avoid signals from large particles to be processed. For each nozzle two histograms are shown. The first histogram was obtained with the discriminator in the off position. All signals are applied to the validation unit. For all nozzles, the second histogram corresponds to an identical position of the amplitude discriminator eliminating signals with high pedestal. These diagrams show that in station A the mean velocity is not affected by amplitude discrimination. The slight differences are within the influence of inlet total pressure which was not exactly constant for these tests. The velocity increase realized in the converging nozzle between the settling chamber and the test section is smooth so that the influence of inertia of droplets with different sizes is limited. When amplitude discrimination is used the only effect seems to be a slight drop in deviation.

Station B is located in front of the upwards going trailing edge shock. Due to important acceleration in the

channel between two adjacent blades, it is to be expected that large and small droplets will have different velocities. Histograms of Fig 9a indicate a much higher deviation than at the cascade inlet. Also the effect of amplitude discrimination is evident (Fig 9b). Signals with high pedestal, generated by large droplets are prevented entering the validation procedure. However, as the intensity distribution in the laser beam is Gaussian, the pedestal amplitude will decrease when the droplet crosses the probe volume away from the central path. As a result of this, the amplitude discriminator is unable to eliminate signals of all large droplets. From Fig 9b it comes out that there are two families of droplets, each of these families corresponding to a Gaussian velocity distribution with different mean values. Fig 9c is a result of data reduction whereby the measurements of the left-most family of Fig 9b are ignored, increasing the mean velocity and decreasing strongly the deviation.

The choice of the nozzle that is to be used for further research is based on the following considerations. As the histograms show that the non-uniformity of the droplets is more pronounced for nozzle N6, this type was rejected. With N3 and N1 additional measurements were performed at several stations along AB (Fig 7). As a result of this, Fig 10 is obtained. Because of the amplitude discriminator does not allow to eliminate a priori signals from droplets of a known diameter, the discriminator is not used for this figure. Examination of the curves led to the choice of N1 for the following reasons :

- in the region of high acceleration, at $5000 < x < 5200$ (see also Fig 1 and 2) the measured velocity increase is more important for nozzle N1.
- when passing through the downwards going trailing edge shock wave ($x < 4200$) a velocity drop is measured with N1 while for N3 the velocity is constant due to inertia of the large droplets.

3.3 Velocity distribution

Along the line AB of Fig 7, the velocity is measured using nozzle N1 for signal generation. At constant cascade inlet pressure, two velocity distributions are obtained, each of them corresponding to a settling chamber temperature so that the condensation shock occurs.

For the first set of measurements no amplitude discrimination is applied, the histograms look like Fig 8a and 9a. As a result of this Fig 11 (AD:0 %) is obtained showing a smooth increase in velocity up to x=5000. For $5000 < x < 4900$ a velocity drop takes place. It is in this region that the condensation shock occurs as indicated on the photographs of Fig 1b and 2b. Large droplets are unable to follow the abrupt velocity drop of the vapour phase, so that the mean velocity only slightly decreases. The same phenomenon occurs at x=4300 when passing through the strong trailing edge shock.

Amplitude discrimination is used for the second velocity distribution. The histograms are similar to those of Fig 8b and 9b. When the same data handling is applied as was done to obtain Fig 9c, considering only those measurements generated by small droplets, the velocity curve is at a much higher level (Fig 11, AD:25 %). The velocity drop due to abrupt condensation is steeper as well as the decrease in velocity when the strong trailing edge shock is crossed. The region of high acceleration, shown on the Schlieren pictures, is also well marked.

4. Conclusion

Optical methods for flow research in air tunnels are usable in steam tunnels providing optimization is sought for the dominant parameters. For visualization techniques the

optical and mechanical properties of the windows are of greatest importance. To apply laservelocimetry each component must be optimized. Seeding must be used as well as high laser power and when it is not monodispersed or when the particles are large, one must be extremely careful. A judicious interpretation of the histograms allows to exclude erroneous measurements.

References

1. DECUYPERE R.

The two-dimensional Steam Tunnel of the Royal Military Academy of Belgium

Measuring Techniques in Transonic and Supersonic Cascade Flow
Proceedings of Symposium at CERL on March 22-23, 1979
Leatherhead

2. DECUYPERE R. - ARTS A.

Influence of the Inlet Conditions on the Blade Pressure Distribution of a Transonic Steam Turbine Tip Section

International Symposium on Applications of Fluid Mechanics and Heat Transfer to Energy and Environmental Problems
Patras - June 1981

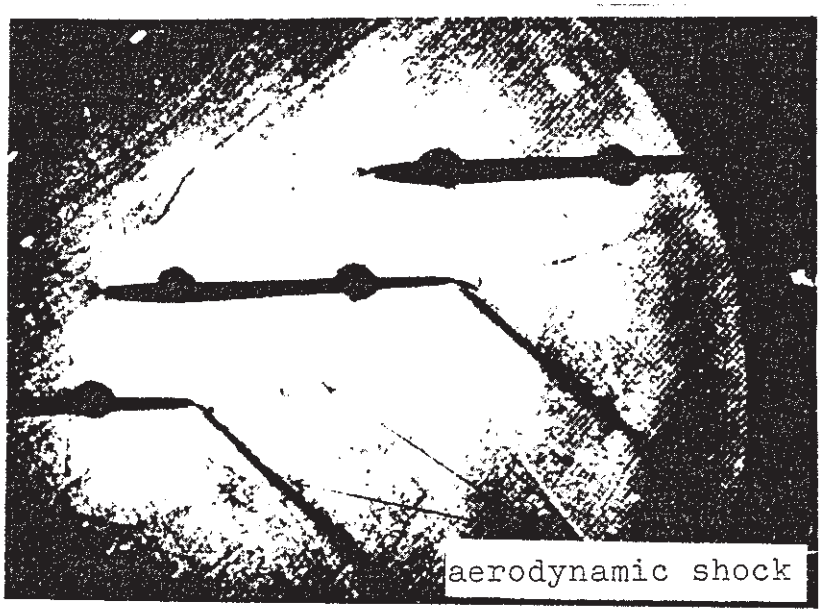

Fig. 1a

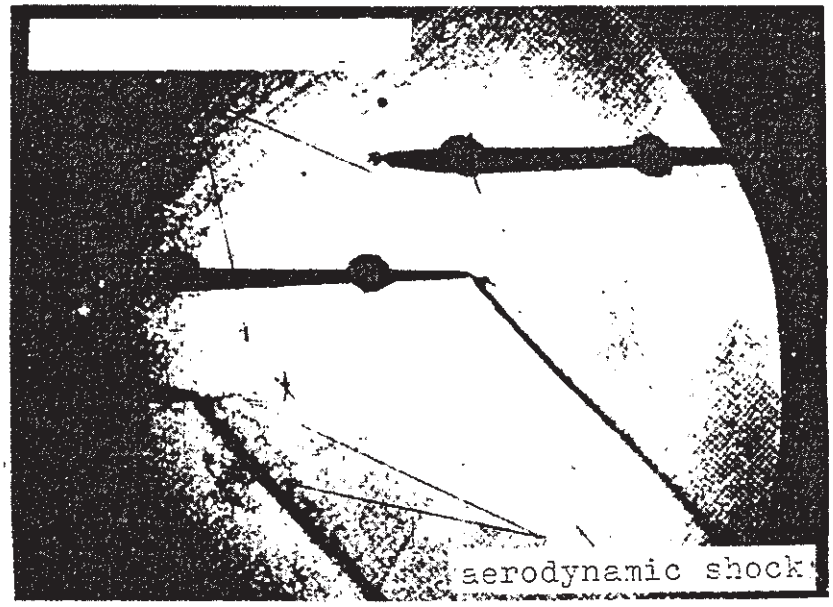

Fig. 1b

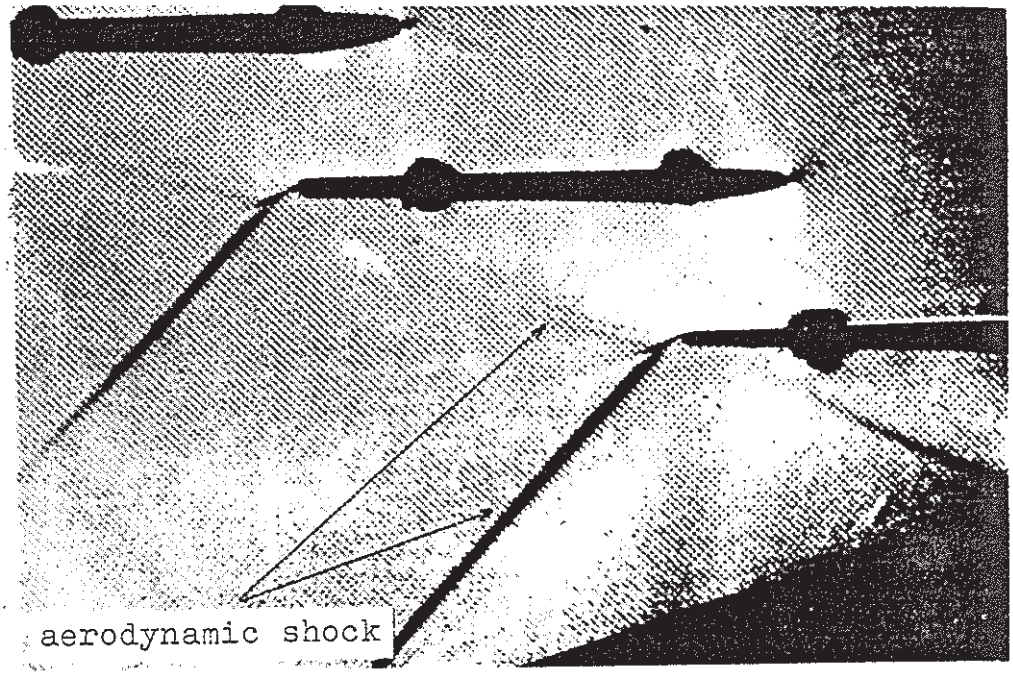

Fig. 2a

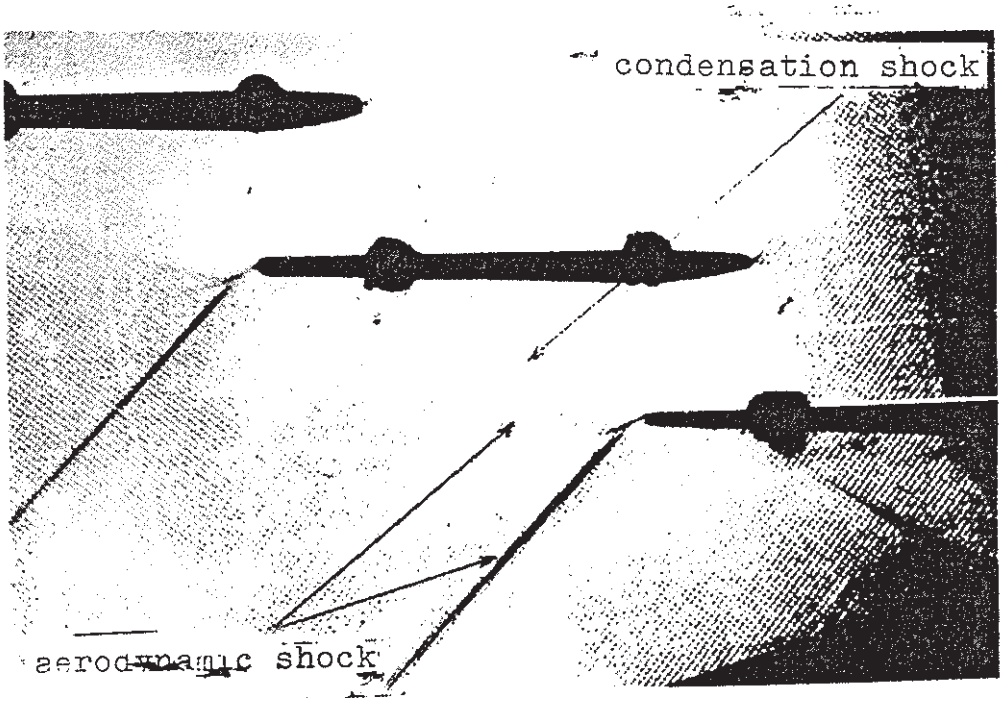

Fig. 2b

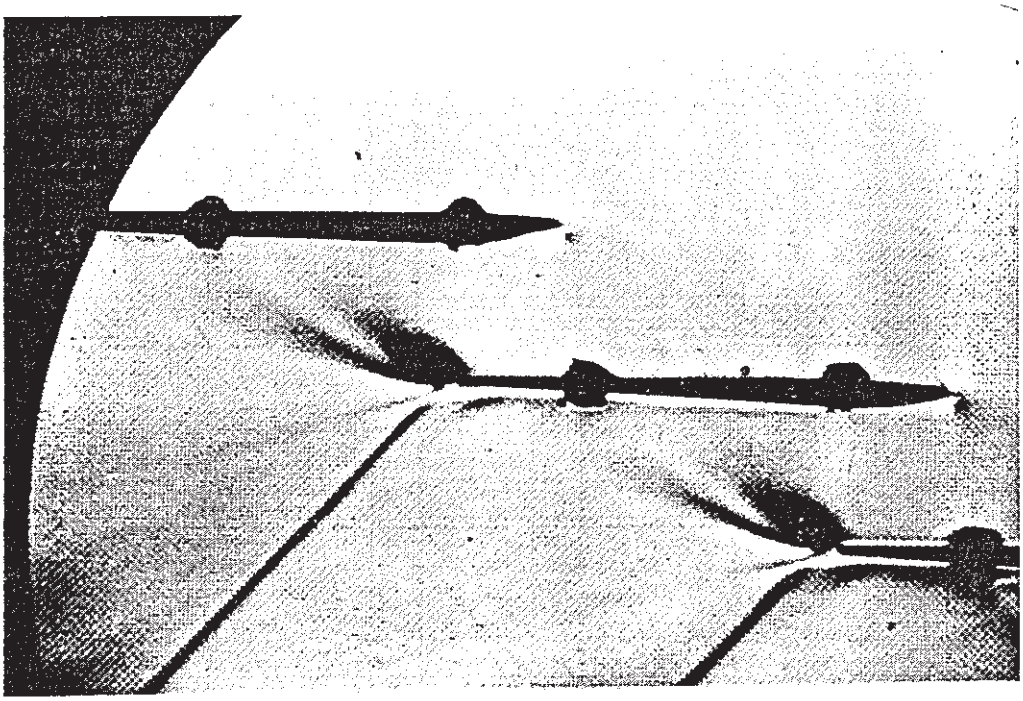

Fig. 3a

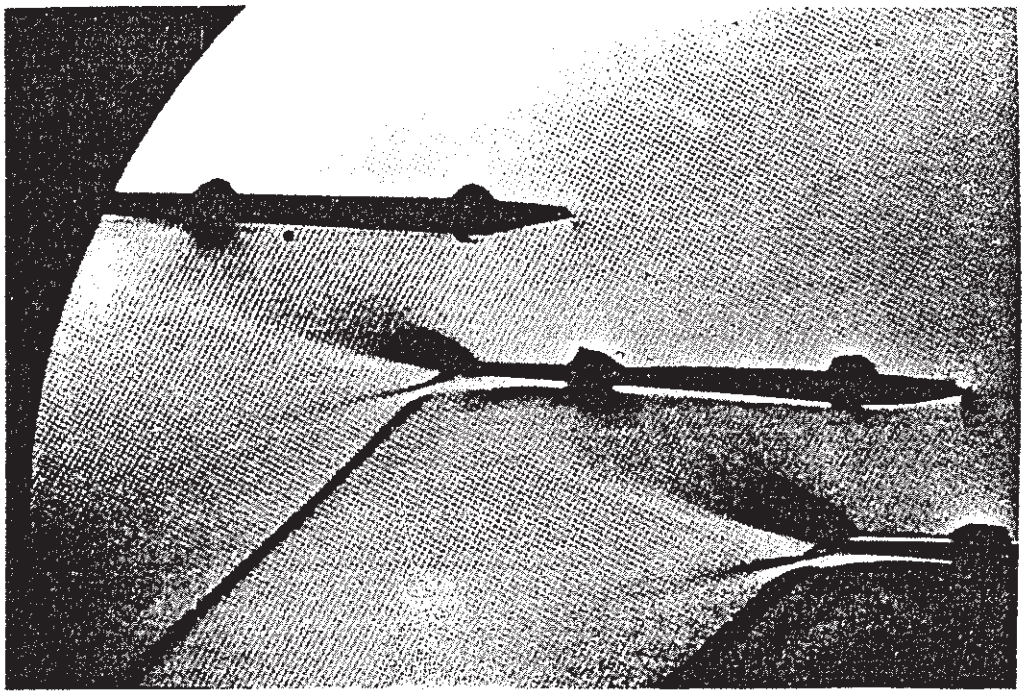

Fig. 3b

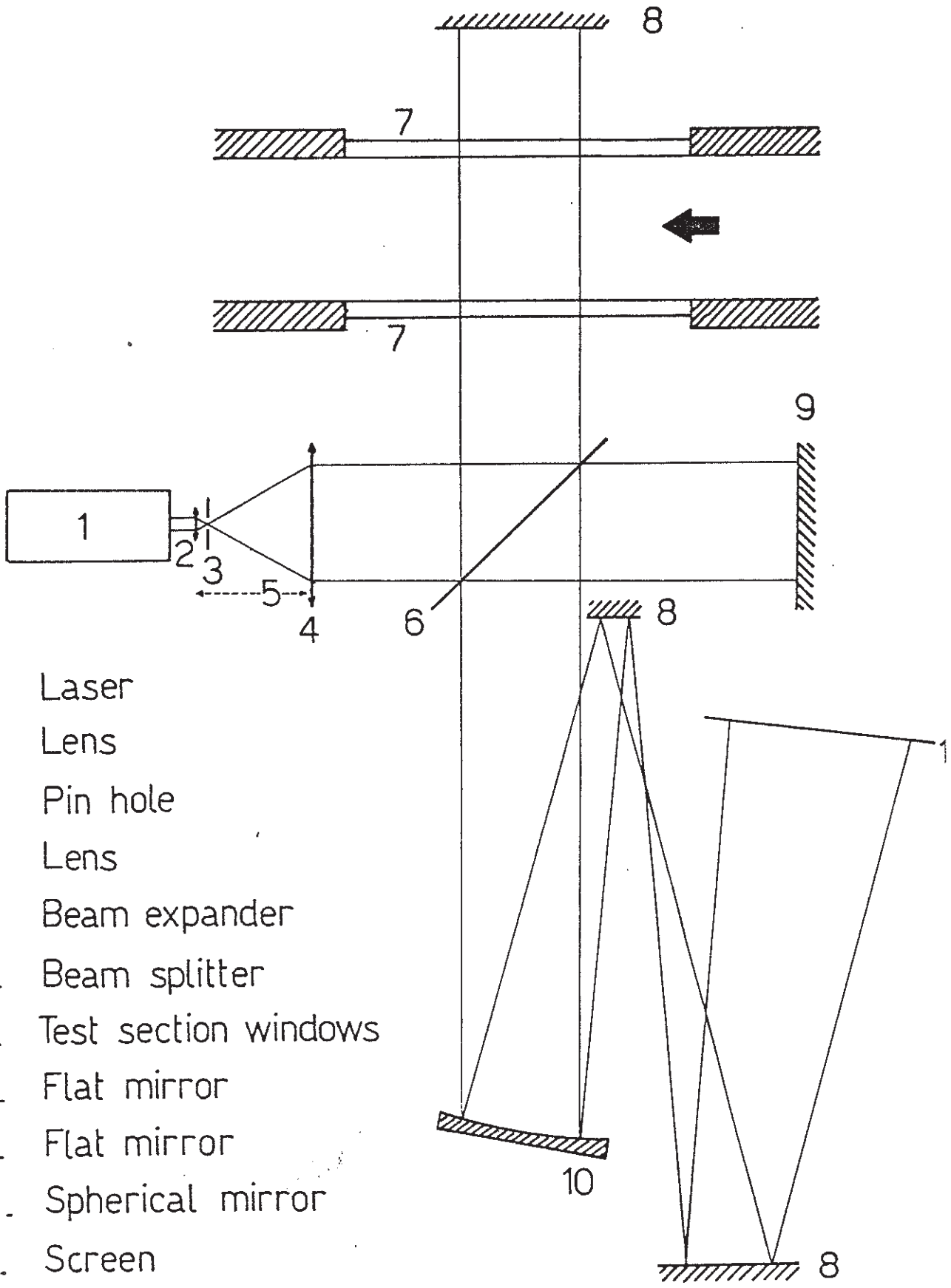

1. Laser
2. Lens
3. Pin hole
4. Lens
5. Beam expander
6. Beam splitter
7. Test section windows
8. Flat mirror
9. Flat mirror
10. Spherical mirror
11. Screen

Fig. 4

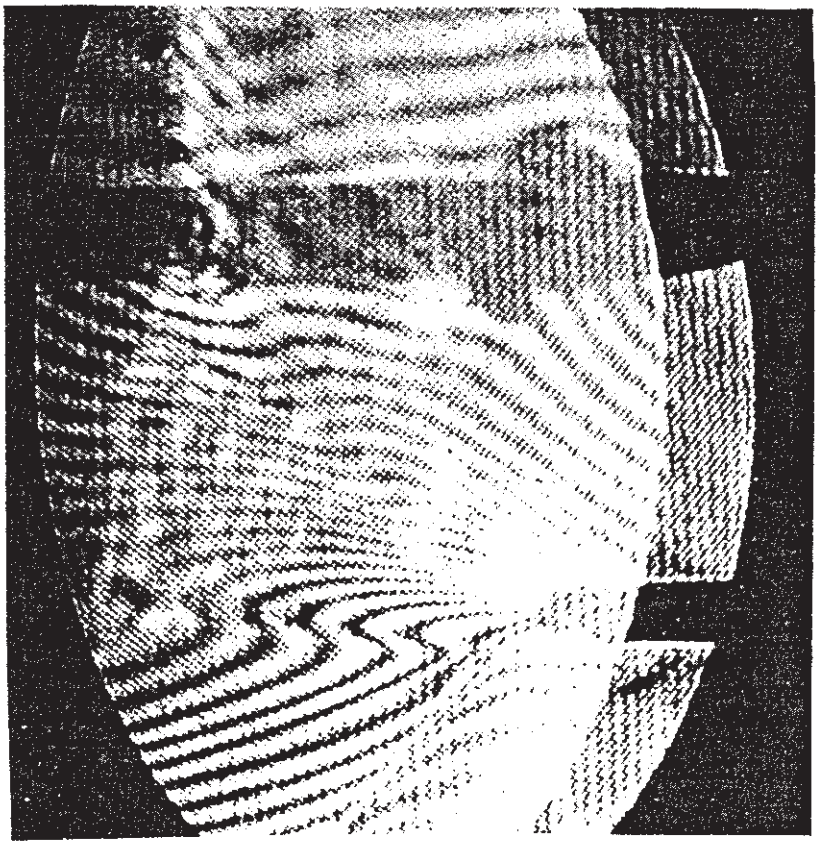

Fig. 5a

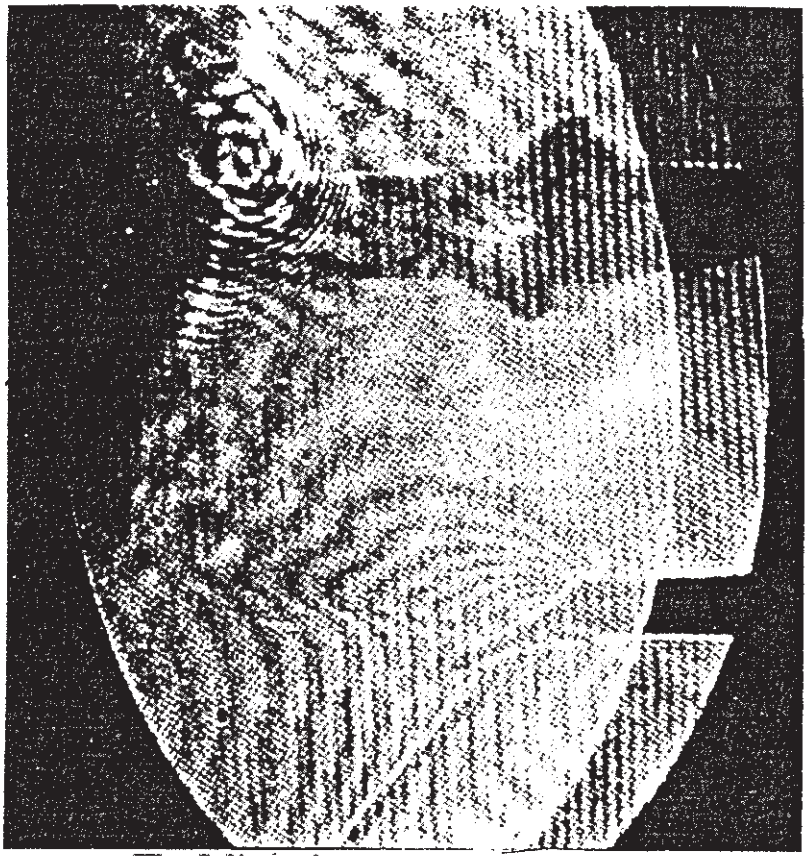

Fig. 5b

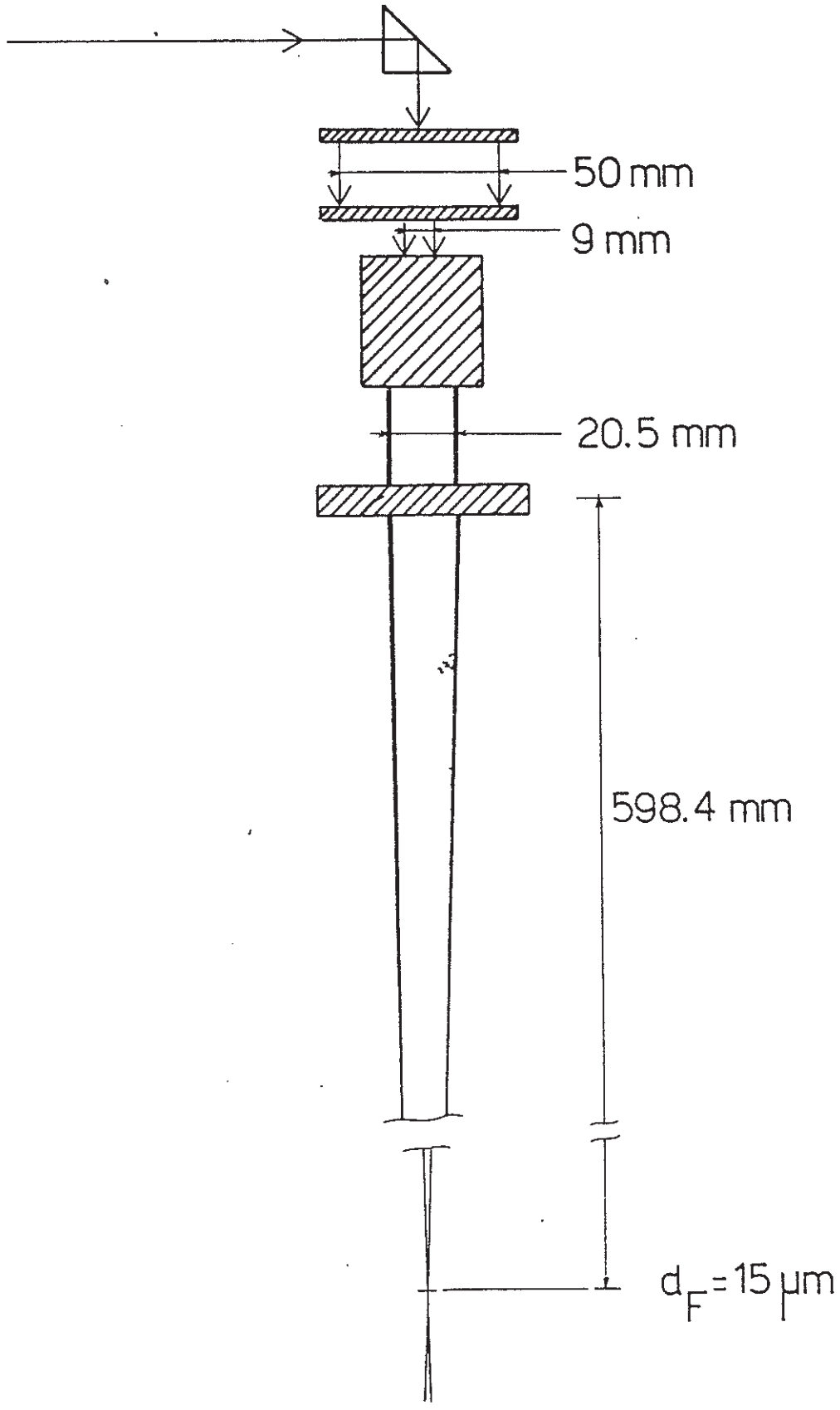

Fig. 6

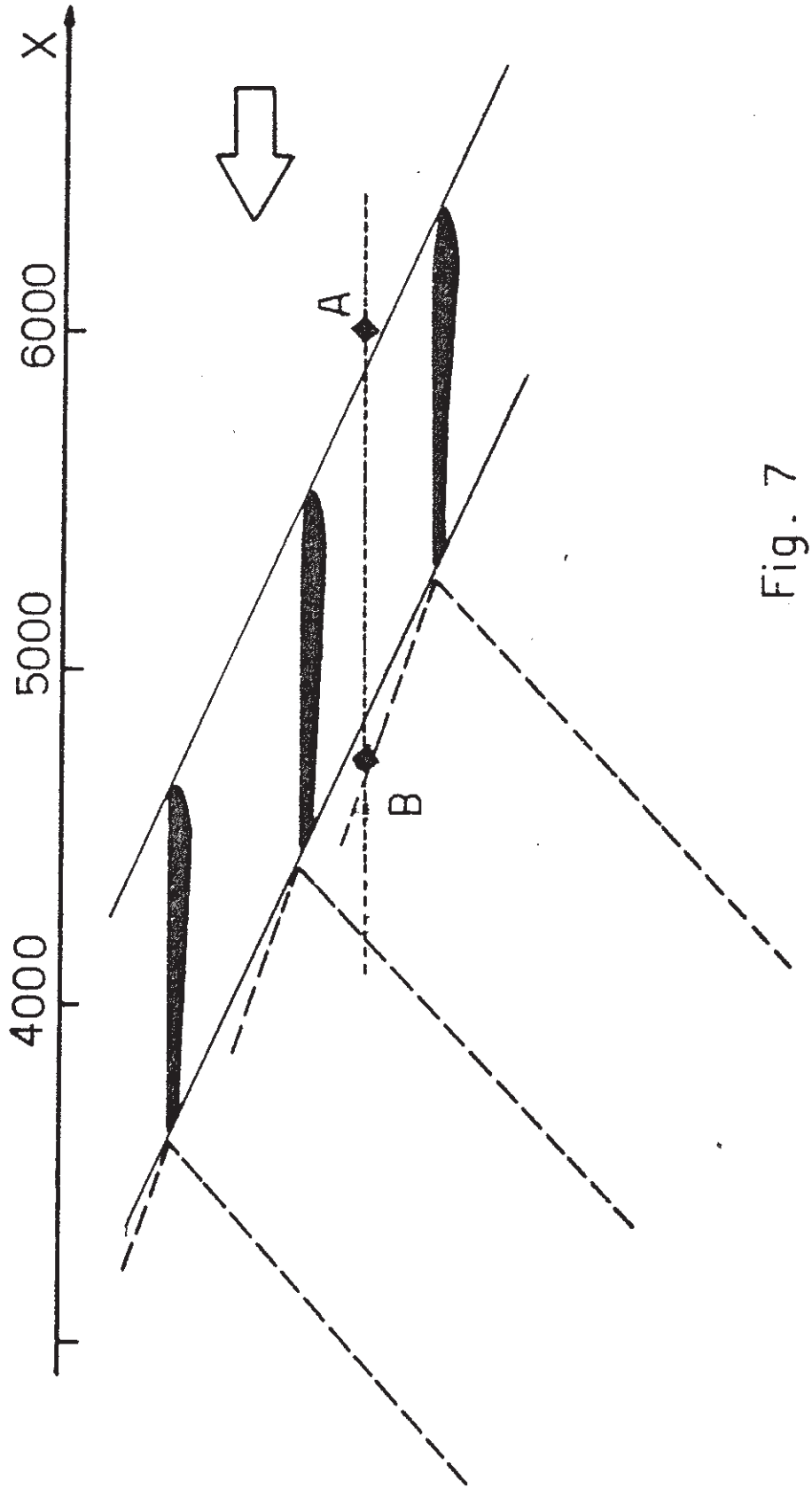

Fig. 7

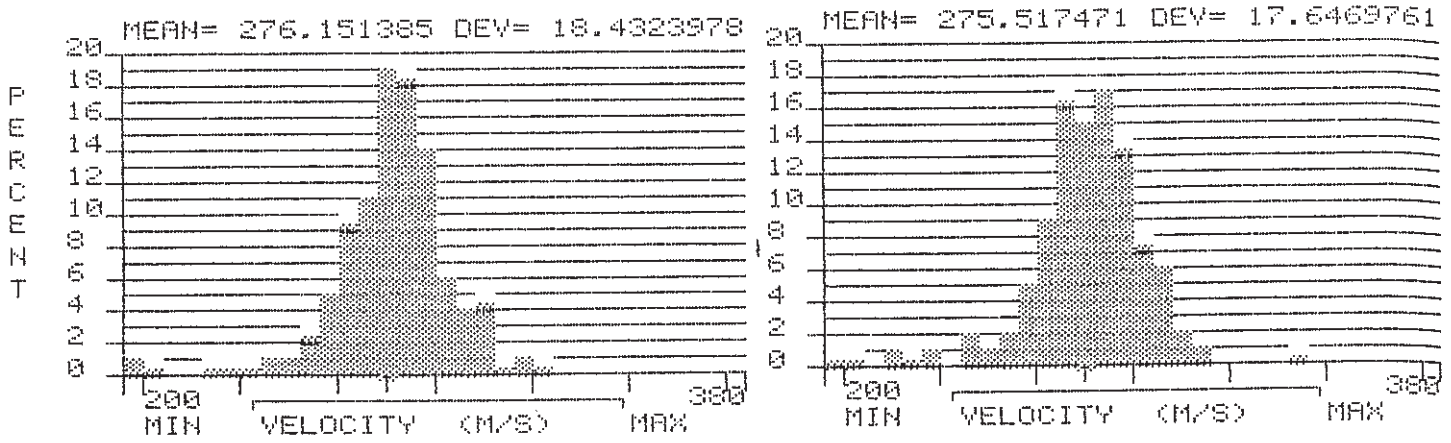

N6

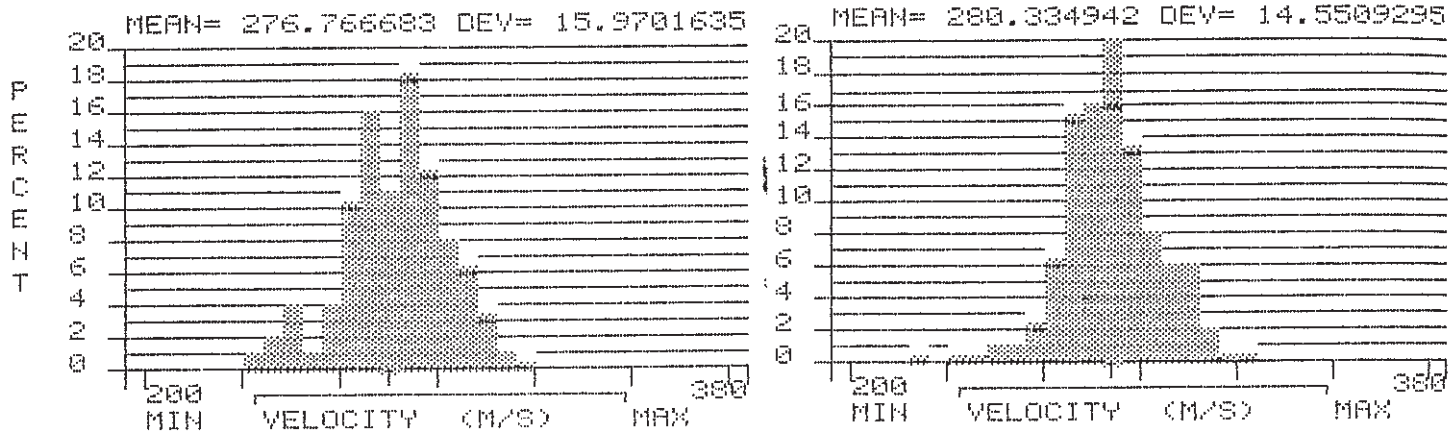

N3

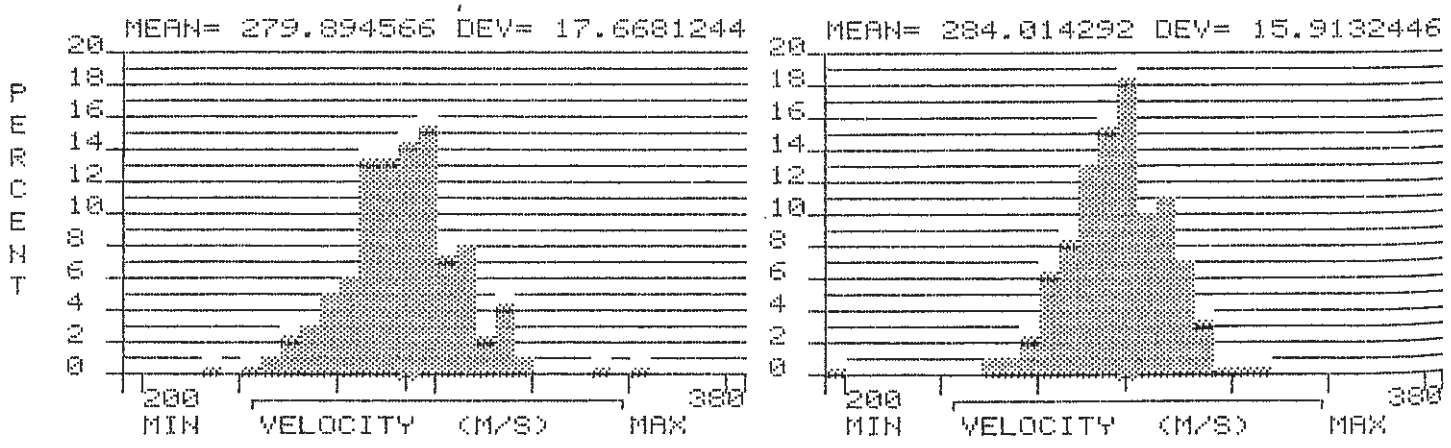

N1

AD = 30%

Fig. 8a

Fig. 8b

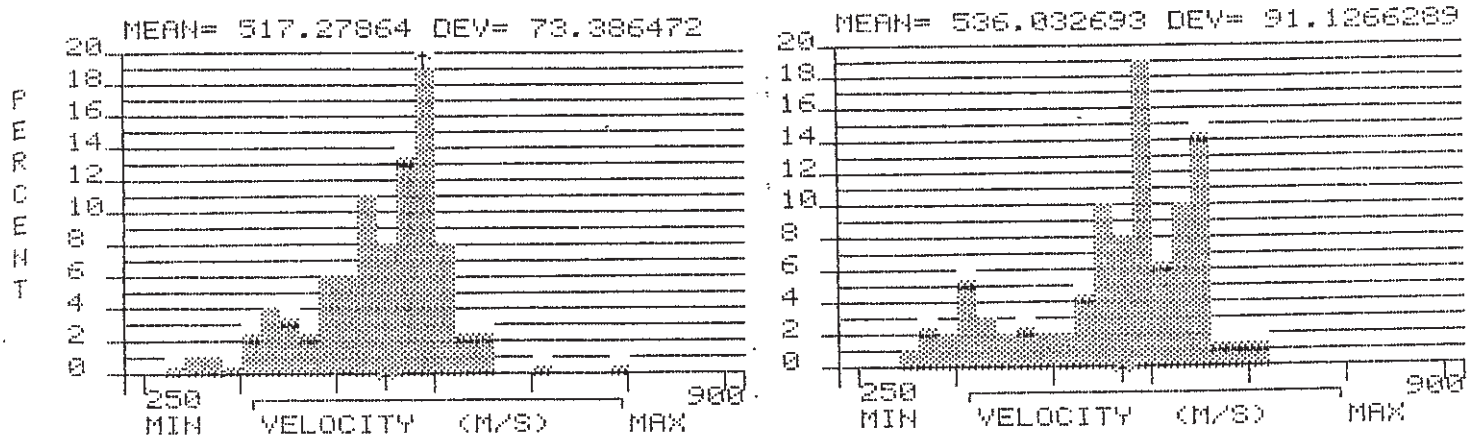

N6

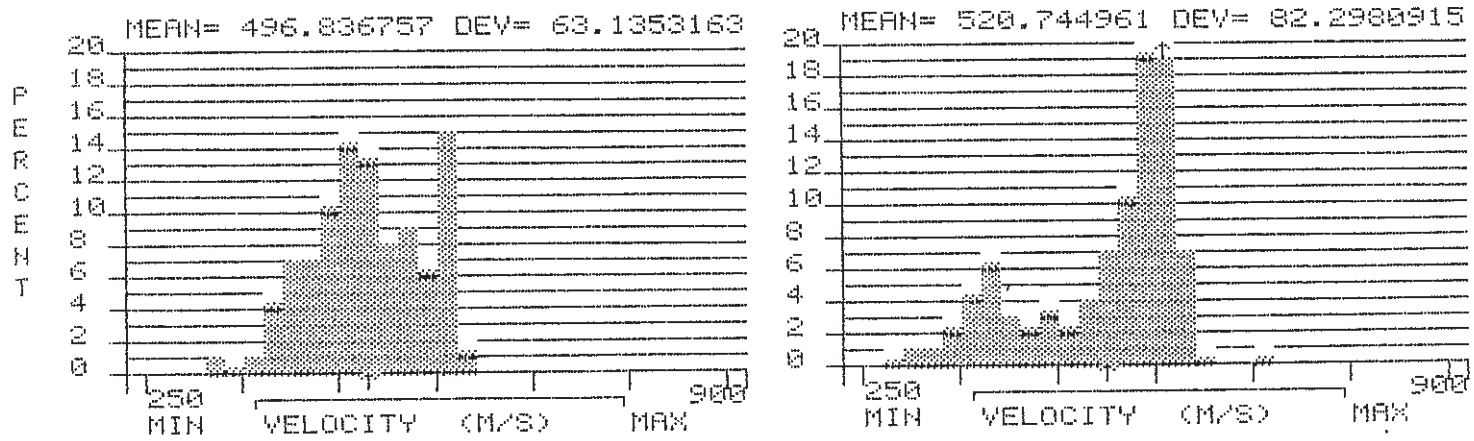

N3

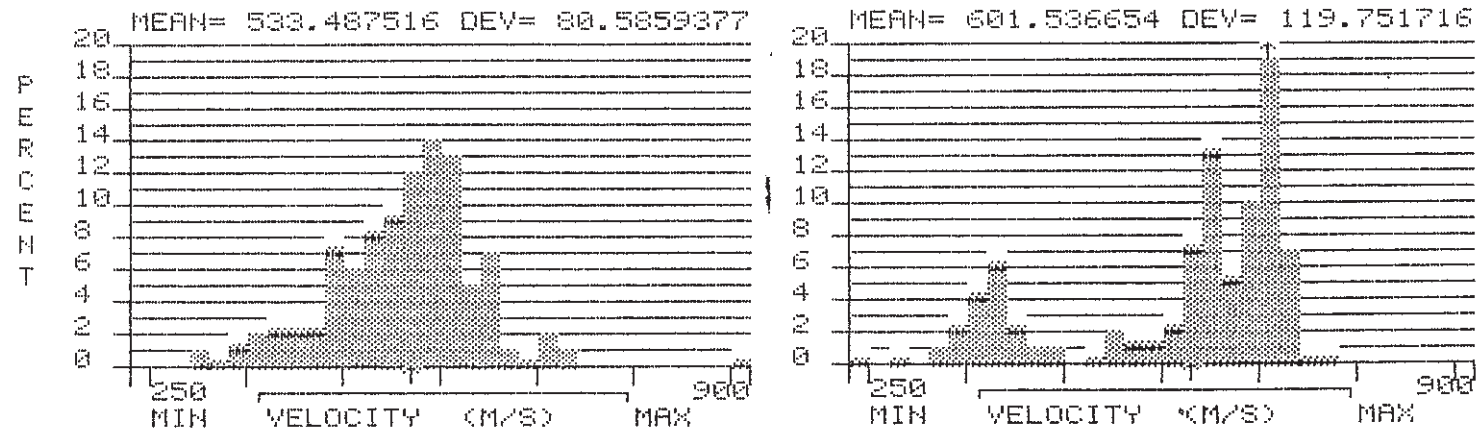

N1

A.D.: 30%

Fig. 9a

Fig. 9b

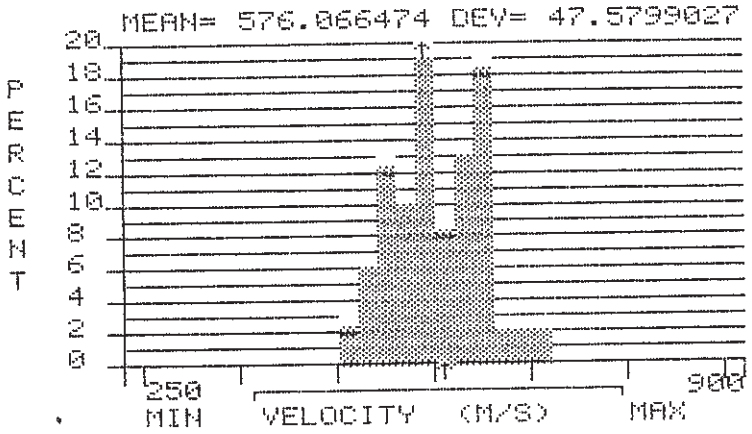

N6

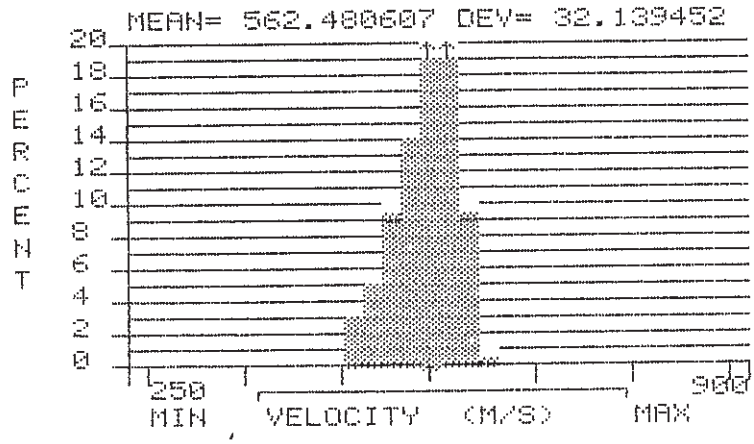

N3

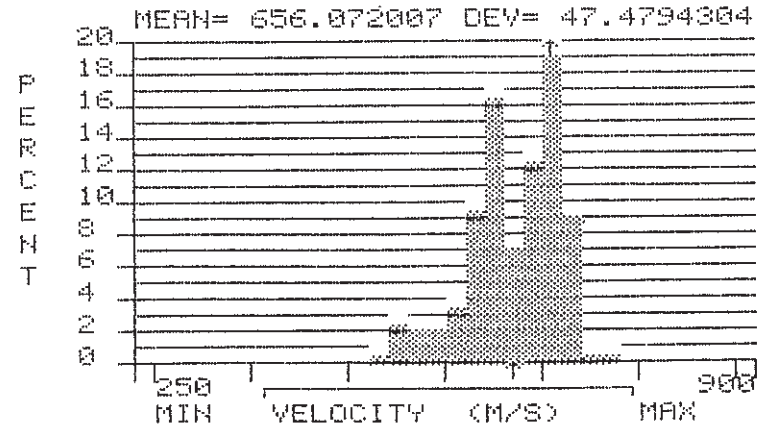

N1

Fig.9c

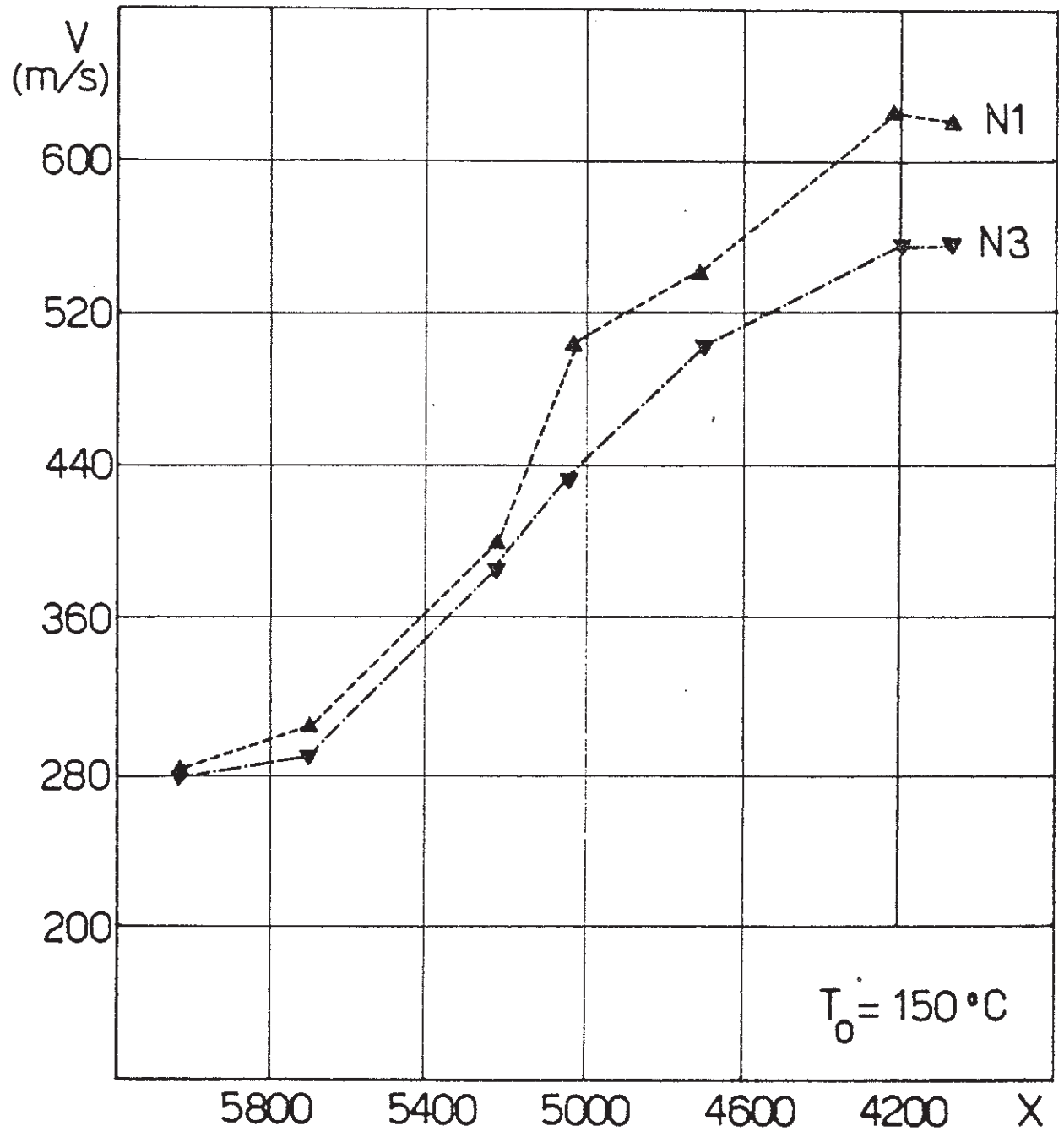
V
(m/s)
600
520
440
360
280
200
N1
N3
T_0 = 150 °C
5800
5400
5000
4600
4200
X

Fig. 10

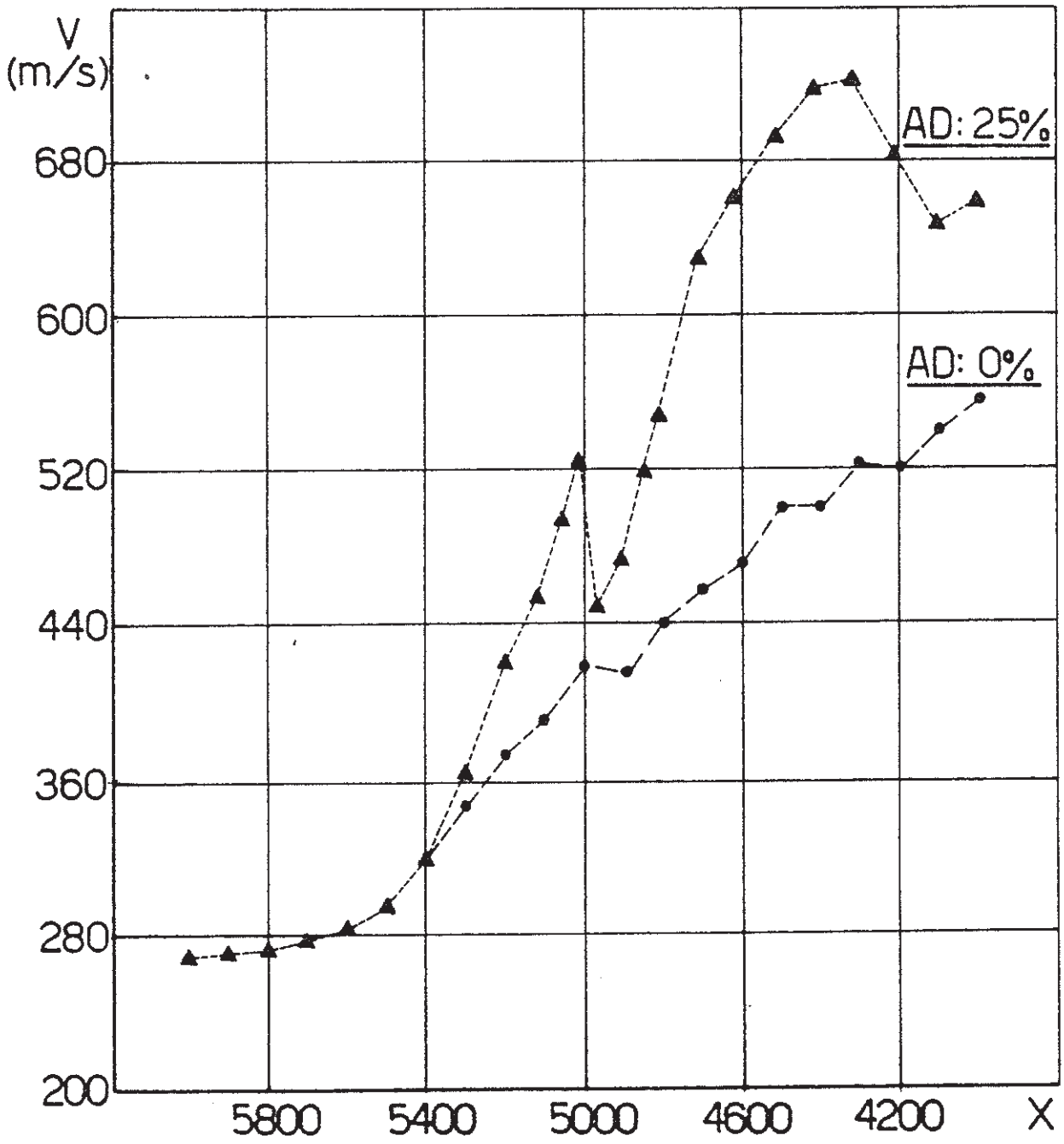
V
(m/s)
680
600
520
440
360
280
200
5800
5400
5000
4600
4200
X
AD: 25%
AD: 0%

Fig. 11